Electronic Supplementary Information

In situ generation of 3D graphene-like networks from cellulose nanofibres in sintered ceramics

Andraž Kocjan[1], Rainer Schmidt[2,3], Ana Lazar[1,4], Jesús Prado-Gonjal[5], Janez Kovač[6], Manca Logar[7], Francisco J. Mompean[3,5], Mar Garcia-Hernandez[3,5] , Eduardo Ruiz-Hitzky[8], Bernd Wicklein[8]**

[1]Department for Nanostructured Materials, Jožef Stefan Institute, Jamova 39, 1000 Ljubljana, Slovenia

[2]Facultad de Ciencias Físicas, GFMC, Universidad Complutense de Madrid, 28040 Madrid, Spain

[3]"Laboratorio de Heteroestructuras con aplicacion en spintronica" Unidad asociada UCM/CSIC, 28049 Madrid, Spain

[4]Jožef Stefan International Postgraduate School, Jamova 39, 1000 Ljubljana, Slovenia

[5]Materials Science Factory, Instituto de Ciencia de Materiales de Madrid (ICMM), Consejo Superior de Investigaciones Científicas (CSIC), Sor Juana Inés de la Cruz 3, 28049 Madrid, Spain

[6]Department for Surface Engineering and Optoelectronics, Jožef Stefan Institute, Jamova 39, 1000 Ljubljana, Slovenia

[7]Department of Materials Chemistry, National Institute of Chemistry, 1000 Ljubljana, Slovenia

[8]Department of New Architectures in Materials Chemistry, Instituto de Ciencia de Materiales de Madrid (ICMM), Consejo Superior de Investigaciones Científicas (CSIC), Sor Juana Inés de la Cruz 3, 28049 Madrid, Spain

*Correspondence to: a.kocjan@ijs.si and/or bernd@icmm.csic.es

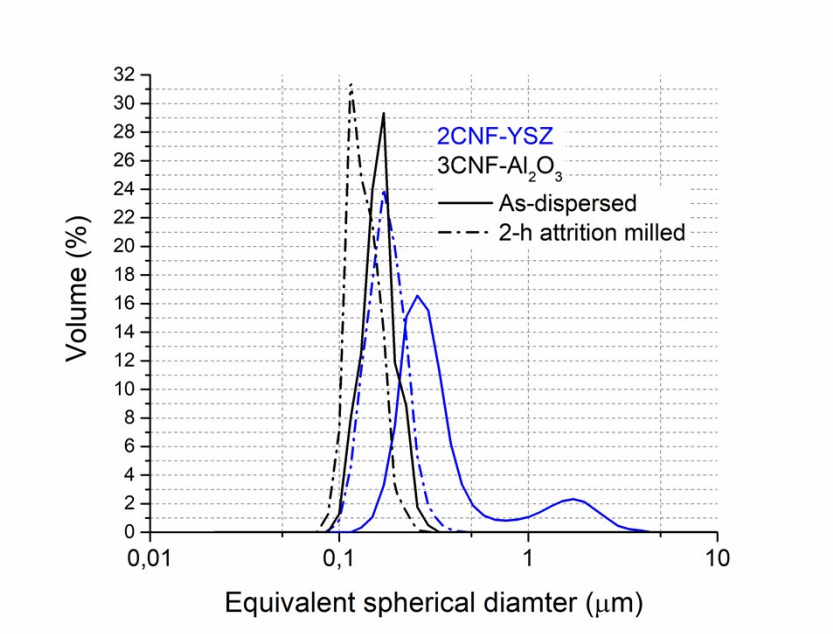

Fig. S1.

Particle size distribution (PSD) of 2%CNF-YSZ and 3%CNF-Al_2O_3 slurries before and after 2-hour attrition milling as measured with laser scattering granulometry. In both cases attrition milling ensured homogeneous and colloidally stable slurries exhibiting a PSD comparable to the provider`s specifications.

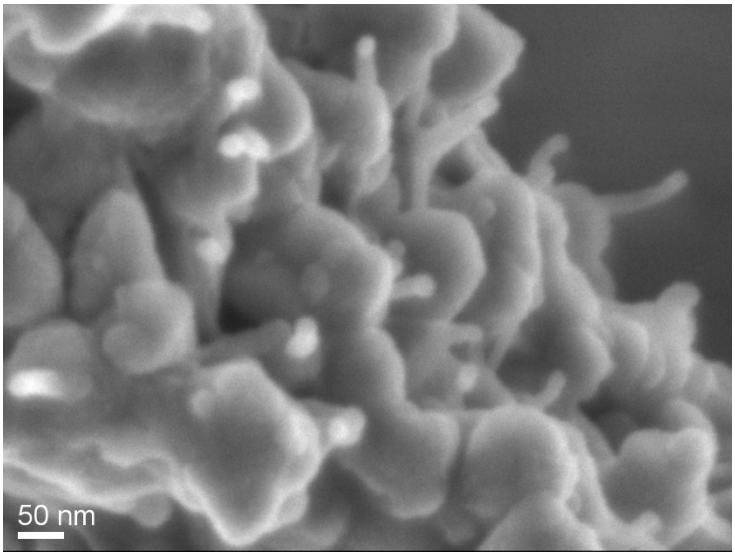

Fig. S2.

SEM image of freeze-dried 3%CNF-Al_2O_3 powder.

Table S1.

Density, flexural green body strength, and grain size of sintered materials as well as mechanical data from Vickers indentation for 2%CNF-YSZ and 3%CNF-Al_2O_3.

	Density (g cm^{-3})		Green strength (MPa)	Grain size (nm)	Vickers indentation	
	Green	SPSed			$H_{v,\ 10\ N}$ (GPa)	K_{ifr} (MPa·$m^{-1/2}$)
2%CNF-YSZ	3.01 (50.2% TD)	6.01±0.03 (99.5% TD)	17.4±0.3	120	14.2±0.38	4.4±0.05
3%CNF-Al_2O_3	2.32 (59.1% TD)	3.96±0.01 (99.8% TD)	15.3±0.5	130	21.2±0.68	4.0±0.14

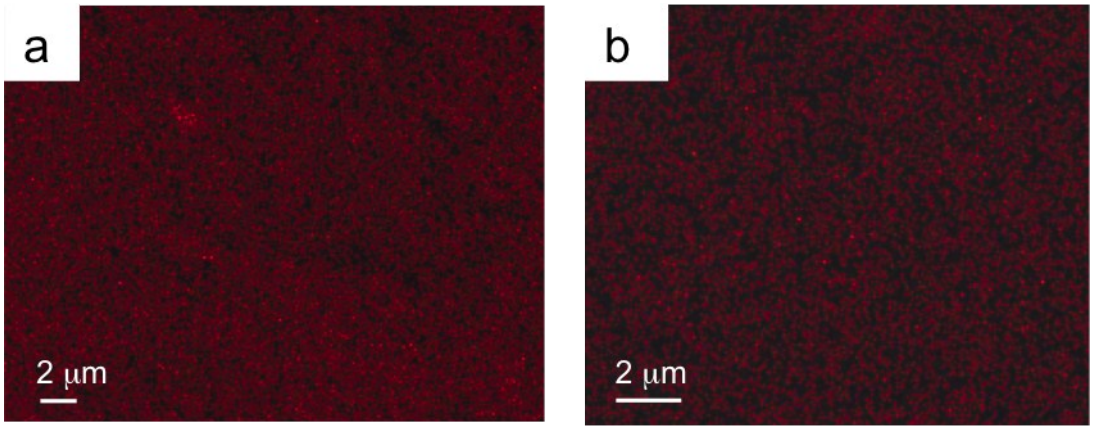

Fig. S3.

EDX carbon mapping of SPS sintered 2%CNF-YSZ (**a**) and 3%CNF-Al_2O_3 (**b**).

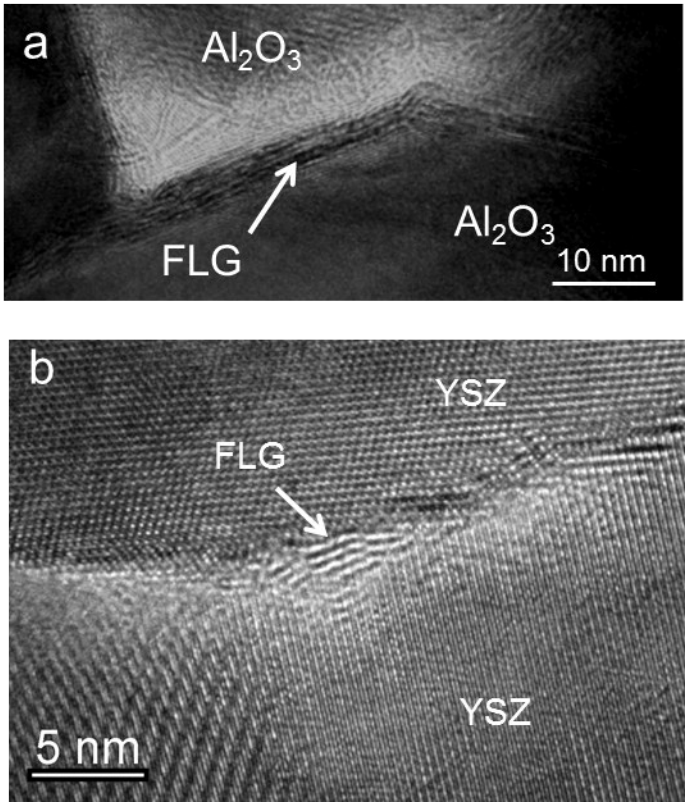

Fig. S4.
TEM images of SPS sintered 3%CNF-Al_2O_3 (**a**) and 2%CNF-YSZ (**b**) showing few layered graphene (FLG) films between Al_2O_3 and YSZ grains, respectively.

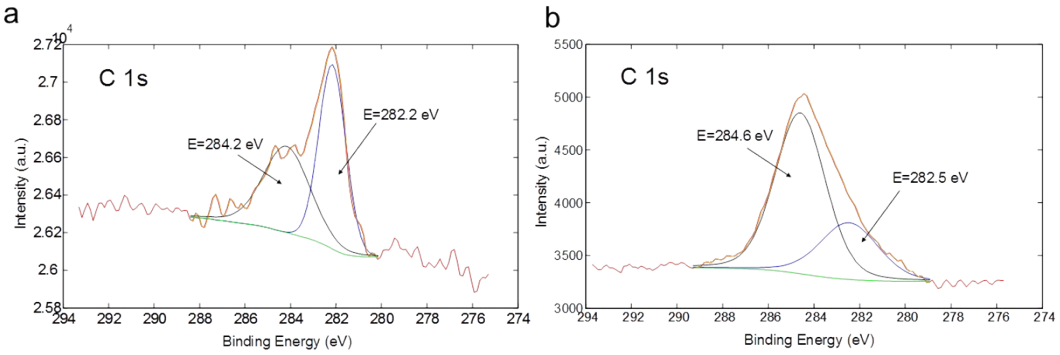

Fig. S5.
XPS core level C 1s spectrum of SPS sintered 2%CNF-YSZ (**a**) and 3%CNF-Al_2O_3 (**b**). The band at 284.6 eV can be attributed to aromatic C-C bonds. The band at 282.0 eV is typical for a carbide phase, however, it was attributed to an artefact due to Ar ion bombardment of carbon species present in ceramics, destroying such species and bonding the recoiled carbon atoms in interstitial positions in the ceramic matrix. The relative intensity of this peak is higher for CNF-YSZ samples compared to CNF-Al_2O_3 samples what was attributed to higher reactivity for carbide formation in the former case. Moreover, there are no indications of C-O bonds in the XPS spectra. This result is in agreement with EELS data that also indicates the absence of oxygen in the carbon

phase (Fig. S7). Therefore, it can be assumed that cellulose was largely reduced to pure carbon at the interface with the ceramic grains.

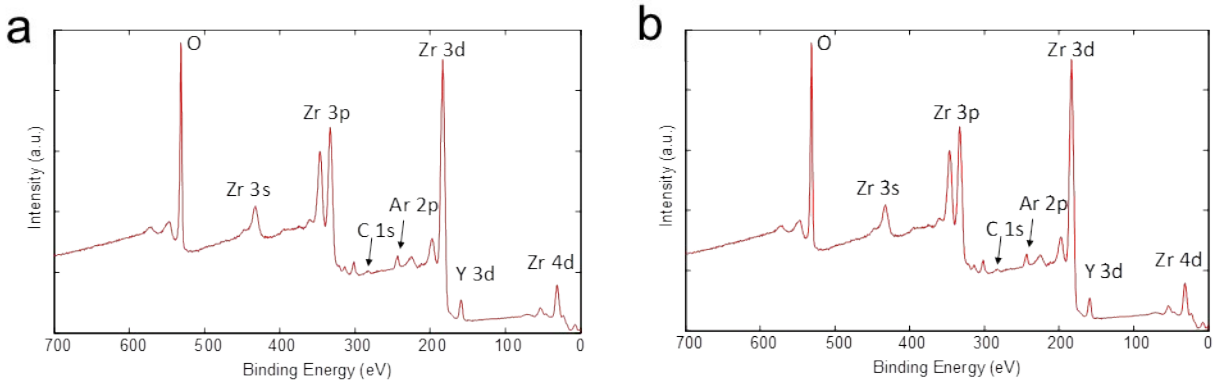

Fig. S6.

XPS wide scan spectra of SPS sintered 2%CNF-YSZ (**a**) and 3%CNF-Al_2O_3 (**b**) obtained during Ar ion bombardment in order to remove surface contamination, from which the carbon content of the samples was quantified.

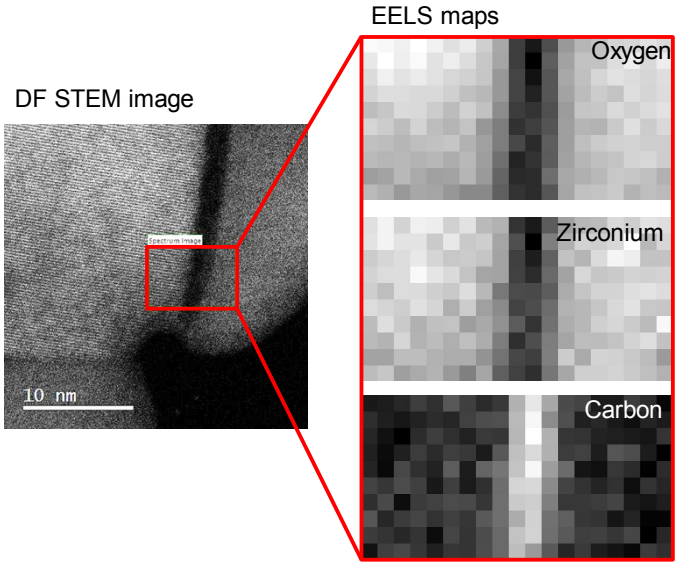

Fig. S7.

DF STEM image of SPS sintered 2%CNF-YSZ and EELS maps across of a grain boundary showing the oxygen (O K_1 edge), zirconium (Zr $M_{4,5}$ edge), and carbon (C K_1 edge) signals. The pixel brightness relates to the signal intensity of the corresponding element, which infers its abundance.

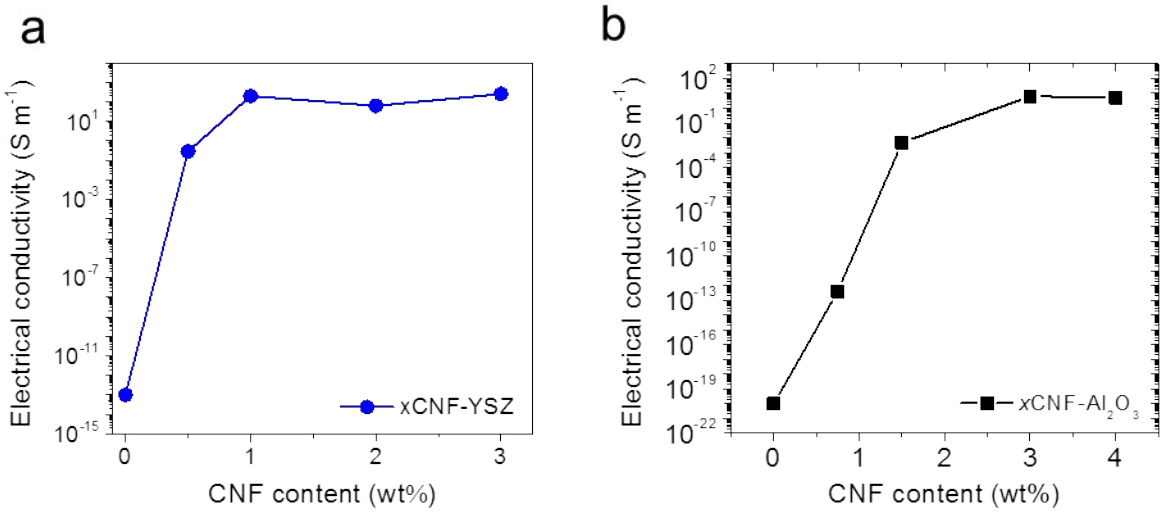

Fig. S8.
Electrical conductivity of SPS sintered *x*CNF-YSZ (**a**) and *x*CNF-Al_2O_3 (**b**) measured at 300 K and 420 K, respectively, as function of the initial CNF content.

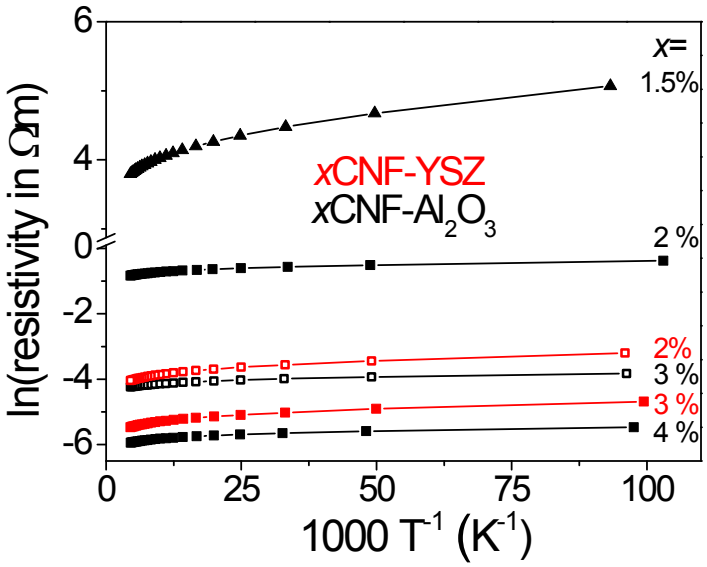

Fig. S9.
Arrhenius plots of the resistivity of SPS sintered *x*CNF-YSZ and *x*CNF-Al_2O_3.

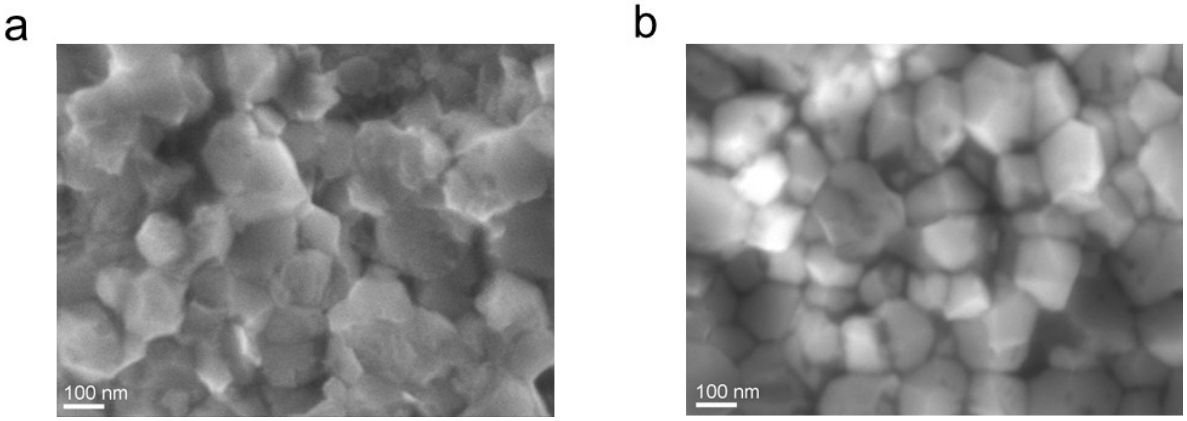

Fig. S10.
SEM micrographs of the fractured surface of SPS sintered 2%CNF-YSZ (**a**) and 3%CNF-Al_2O_3 (**b**)

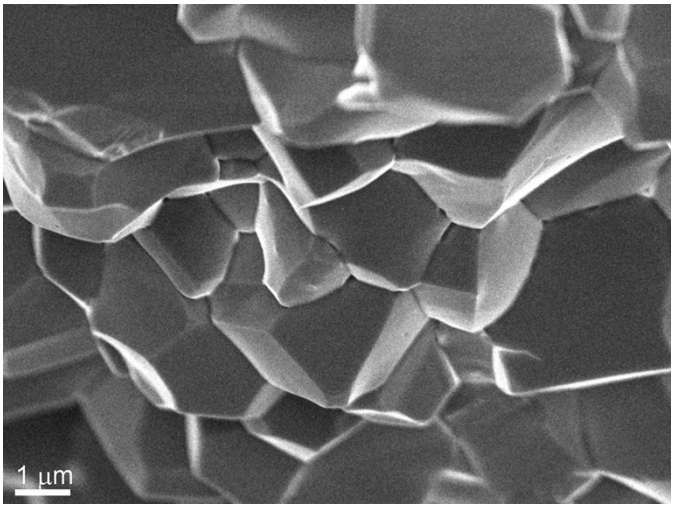

Fig. S11.
SEM micrograph of fractured surface of SPS sintered pure Al_2O_3 using the same sintering program as for 3%CNF-Al_2O_3.

The SEM images in Fig. S10 show that sintered 2%CNF-YSZ and 3%CNF-Al_2O_3 ceramics do not undergo any substantial grain growth as compared to the size of the initial powders (Fig. 1b, Fig. S2). The initial average crystallite size of the powders was 100-200 nm, which persists in the sintered composite ceramics (Table S1), but increases by more than one order of magnitude in sintered pure alumina (Fig. S11).